

Compact, high-repetition rate OPCPA system for high harmonic generation

Jan Matyschok,^{a,b,*} Thomas Binhammer,^b Tino Lang,^{a,c} Oliver Prochnow,^b Stefan Rausch,^b Piotr Rudawski,^d Anne Harth,^{a,c,d} Miguel Miranda,^d Chen Guo,^d Eleonora Lorek,^d Johan Mauritsson,^d Cord L. Arnold,^d Anne L'Huillier,^d and Uwe Morgner^{a,c,e}

^a Institute of Quantum Optics, Leibniz Universität Hannover, Welfengarten 1, D-30167 Hannover, Germany; ^b VENTEON Laser Technologies GmbH, Hertzstraße 1b, D-30827 Garbsen, Germany; ^c Centre for Quantum Engineering and Space-Time Research (QUEST), Welfengarten 1, D-30167 Hannover, Germany; ^d Department of Physics, Lund University, P.O. Box 118, SE-221 00 Lund, Sweden; ^e Laser Zentrum Hannover (LZH), Hollerithallee 8, D-30419 Hannover, Germany

*matyschok@iqo.uni-hannover.de

ABSTRACT

A compact, high-repetition rate optical parametric chirped pulse amplifier system emitting CEP-stable, few-cycle pulses with 10 μJ of pulse energy is reported for the purpose of high-order harmonic generation. The system is seeded from a commercially available, CEP-stabilized Ti:sapphire oscillator, delivering an octave-spanning spectrum from 600-1200 nm. The oscillator output serves on the one hand as broadband signal for the parametric amplification process and on the other hand as narrowband seed for an Ytterbium-based fiber preamplifier with subsequent main amplifiers and frequency doubling. Broadband parametric amplification up to 17 μJ at 200 kHz repetition rate was achieved in two 5 mm BBO crystals using non-collinear phase matching in the Poynting-vector-walk-off geometry. Efficient pulse compression down to 6.3 fs is achieved with chirped mirrors leading to a peak power exceeding 800 MW. We observed after warm-up time a stability of $< 0.5\%$ rms over 100 min. Drifts of the CE-phase in the parametric amplifier part could be compensated by a slow feedback to the set point of the oscillator phase lock. The CEP stability was measured to be better than 80 mrad over 15 min (3 ms integration time).

The experimentally observed output spectra and energies could be well reproduced by simulations of the parametric amplification process based on a (2+1)-dimensional nonlinear propagation code, providing important insight for future repetition rate scaling of OPCPA systems. The system is well-suited for attosecond science experiments which benefit from the high repetition rate. First results for high-order harmonic generation in argon will be presented.

Keywords: OPCPA, parametric amplification, few-cycle, CEP-stable, HHG

1. INTRODUCTION

Applications requiring intense few-cycle laser pulses with a stable Carrier Envelope Phase (CEP) are in the focus of current research. The workhorses during the last ten years, especially in the field of High-order Harmonic Generation (HHG) and attosecond physics, were Ti:sapphire-based Chirped-Pulse Amplifier (CPA) systems with subsequent pulse compression stages. However, this type of systems meanwhile has reached some limitations for further scaling of average power or repetition rate. As an alternative approach, Optical Parametric Chirped-Pulse Amplification (OPCPA) systems [1, 2] are experiencing an increased momentum of development. Such amplifier systems are scalable in terms of output power and repetition rate and directly provide a broad amplification bandwidth in a variety of wavelength regimes from the visible to the mid-infrared [3-5]. Direct amplification of few-cycle laser pulses into the mJ-regime [6, 7] has been shown at low repetition rates. With this amplification concept even the single-cycle limit comes into reach and pulse durations well below 5 fs have been demonstrated [8, 9] by combining several Optical Parametric Amplifier (OPA) stages. At high repetition rates in the range from 100 kHz up to 1 MHz some multi- μJ systems have been reported [10-13], emitting up to 22 W of average power with sophisticated laboratory set-ups [14]. Many experimental applications (e.g. photoemission electron microscopy [15] or coincidence detection of photoelectrons [16]) will benefit from a higher repetition rate due to shorter integration times, higher photon flux, and increased statistics. Recently, CEP dependent

HHG cutoff spectra [17] have been observed from a CEP-stable, few-cycle OPCPA system operated above 100 kHz, indicating the generation of an isolated attosecond pulse. This experiment demonstrates the potential of OPCPA technology and highlights the importance of CEP stability for applications such as HHG [18] or photoionization [19]. Due to the complexity of experiments for XUV and attosecond spectroscopy, there is a strong need for user-friendly, reliable and long-term stable light sources.

In this paper we present a compact OPCPA system delivering at 200 kHz repetition rate, CEP-stable sub-7 fs pulses with energies exceeding 10 μ J. The setup is designed for maximum compactness, low complexity, and low noise in order to bring the OPCPA technology to the next step towards compact and reliable light sources, ideally suited for many types of nonlinear light-matter interaction experiments. A CEP stabilized octave-spanning seed oscillator provides, without further nonlinear spectral shifting, the ultra-broadband signal and the narrowband seed for the Yb-based pump amplifier. The frequency doubled amplifier outputs pump two subsequent broadband Non-collinear Optical Parametric Amplifier (NOPA) stages. The parametric amplification process could be well reproduced with the help of our (2+1) dimensional propagation code [20]. In our previous publication [13] various experimentally observed spatial phenomena occurring along with the NOPA in the chosen Poynting-Vector-Walk-off Compensation (PVWC) geometry were investigated and compared to the experimental results. In the current work, we present high-order harmonic generation in argon demonstrating the usability of this OPCPA system for XUV applications at high-repetition rates.

2. EXPERIMENTAL SETUP AND RESULTS

In Fig.1 an overview of the OPCPA system is given. The setup consists of a CEP stabilized broadband Ti:sapphire oscillator, an ytterbium doped fiber preamplifier seeding two separate rod-type fiber amplifiers, pump pulse compression with subsequent Second Harmonic Generation (SHG), two NOPA stages followed by a chirped mirror compressor, and an f-to-2f interferometer. The system is boxed to reduce CEP and amplitude noise and fits on a compact footprint (150 x 210 cm). The broadband Ti:sapphire oscillator (VENTEON | PULSE : ONE OPCPA SEED) delivers an pulse energy of 3 nJ at 80 MHz with an octave spanning spectrum from 600 nm – 1200 nm. The CEP beat signal was detected with a self-referencing f-to-2f interferometer using the outer edges of the oscillator spectrum after a dichroitic filter mirror. The filtering for the CEP locking reduces the output power from the oscillator by less than 10 %. The feedback to the oscillator is realized by pump power modulation via an acousto-optic modulator, whereas slow drifts are compensated by changing the position of the intra-cavity wedge pair with a motorized stage. This concept enables a long-term locking for more than 12 hours, with a low rms phase noise of 80 mrad (3 Hz – 1 MHz). Due to the large fundamental oscillator bandwidth no external spectral shifting (e.g. in nonlinear fibers) is required to reach sufficient seed energy around 1030 nm for the fiber amplifier, which greatly enhances the noise performance and long-term stability of the amplifier seed. Furthermore, no coupling or soliton effects are affecting the timing jitter between pump and signal pulses of the OPCPA, which is especially crucial when using pump pulse durations in the range of several hundreds of fs. After filtering, the oscillator output still supports sub-6 fs pulses, with 2.5 nJ pulse energy and is used as signal radiation for the first NOPA stage.

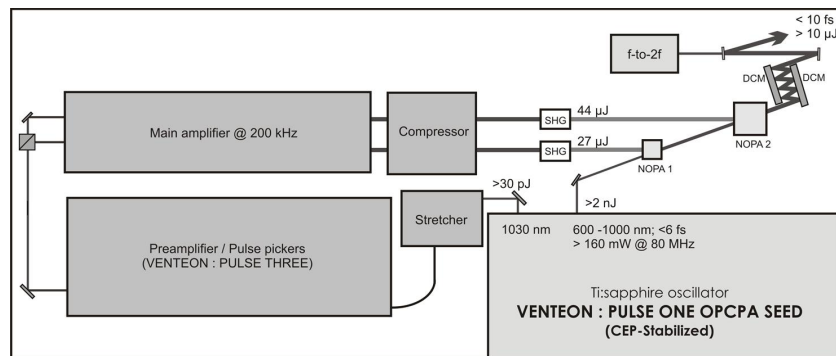


Fig. 1 Experimental setup of the OPCPA system: SHG: Second Harmonic Generation; NOPA: Non-collinear Optical Parametric Amplifier; DCM: Double Chirped Mirrors; f-to-2f: interferometer for the carrier envelope phase measurement.

The infrared light, centered at 1030 nm, was separated by a dichroic mirror from the broadband oscillator spectrum and temporally stretched by a Chirped Volume Bragg Grating (CVBG, 27 ps/nm, 16 nm FWHM) to several hundreds of

ps. The benefits of this approach are the small footprint of the stretcher arrangement, which can be implemented within the oscillator housing, and the monolithic and thereby drift-free design. After temporal stretching, amplification to about 300 mW at 200 kHz repetition rate takes place in a three-stage fiber preamplifier chain, including two pulse pickers. The output of the preamplifier is divided into two beam lines for seeding two separate Rod-type fibers (NKT, DC 285/100 PM-Yb-ROD, 80 cm long) for high power amplification. The advantage of this parallel concept is the reduced average power and pulse energy in each power amplification stage compared to a one-stage amplifier. Furthermore, the pump pulse energies and pulse durations for the two NOPA stages could be adapted independently to optimal performance. Each fiber main amplifier delivers pulse energies of around 100 μJ before compression. In the current case, the stretched pulse duration limits the pulse energy in the fiber amplifiers due to nonlinear effects. As in the present implementation the focus was on compactness and reduced complexity of the stretcher unit, further energy scaling could be realized in the future by implementing a different stretching concept, e.g. with a much less compact and stable grating sequences. Pulse compression was performed in the first stage with an efficiency of 57 % by a second CVBG matched to the used stretcher. Compression of the second stage was realized by a GRISM instead of a designated third CVBG due to the higher efficiency (67 %) together with the better pulse and beam quality. After frequency doubling, pump energies of 27 μJ are observed for the first stage and 44 μJ for the second stage, with pulse durations of around 500 fs.

Broadband parametric amplification of the seed pulses is achieved by non-collinear interaction of pump and signal beam in the two BBO crystals. For the first parametric amplification stage an internal angle between signal and pump of 2.4° was used to achieve the most broadband phase matching. For the available pump energy of 27 μJ , a crystal length of 5 mm was chosen in the PVWC geometry. Here amplification from 1.25 nJ (at 80 MHz) up to 4.5 μJ (at 200 kHz) was achieved with a $1/e^2$ -beam radius of 175 μm for the pump and a slightly smaller radius of 110 μm for the signal. Due to the dispersion of glass, air, and BBO the signal pulse after the first stage is stretched to 420 fs pulse duration (measured with VENTEON | PULSE : FOUR SPIDER). In between the NOPA stages the positive chirp of the seed is slightly reduced by using two bounces on a chirped mirror pair (VENTEON, 600-1200 nm, -120 fs^2 / pair at 800 nm).

The second NOPA (5 mm BBO) is operated in the same phase matching geometry and seeded with approximately 270 fs input pulse duration and 3.4 μJ pulse energy, focused down to 170 μm radius spot size. To avoid crystal damages a slightly larger spot size of 270 μm was chosen for the 44 μJ pump energy to keep the intensity on the BBO crystal below 100 GW/cm^2 . In this stage, an optical-to-optical power conversion efficiency of 31 % from pump to signal leads to an amplification to up to 17 μJ . The spectral bandwidth of more than 450 nm (at -10 dBc, see Fig. 2(a)) after the second NOPA supports a pulse duration of 4.9 fs. Due to the moderate stretching of the broadband signal, pulse compression with an overall throughput above 80 % is possible using a simple, compact, and drift-free chirped mirror compressor with 12 reflections in double-pass configuration. The mirror dispersion is designed for compensation of the BBO crystal, air, and fused silica. The pulse duration after compression is measured to be as short as 6.3 fs (see Fig. 2(b)) using SPIDER.

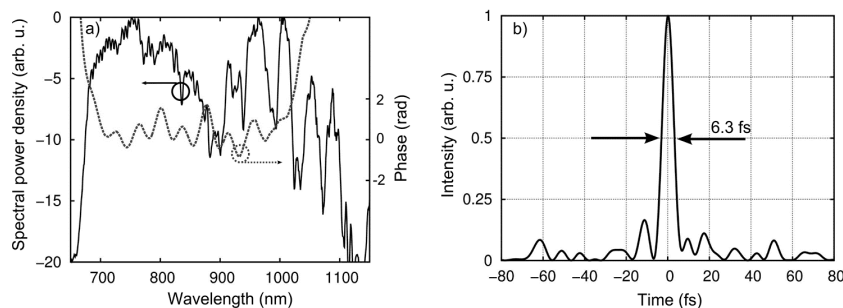


Fig. 2 a) Measured spectrum from the compressed pulse after the second NOPA stage (black) together with the spectral phase (dotted black) from the SPIDER measurement. b) Reconstructed pulse from the SPIDER measurement.

A small fraction (approx. 300 nJ) of the compressed output beam is separated and sent to an f-to-2f interferometer. The interference pattern was recorded by using an USB-spectrometer (Avantes AVASPEC-2048-USB2), and allows determining directly the CEP stability of the OPCPA system output. The spectra were recorded with 3 ms integration time and an average over 10 spectra respectively. A slow phase drift was obtained with open feedback loop (see Fig.3(a)). By closing the feedback loop for thermal drift compensation, an excellent stability of 68 mrad over 15 min could be reached (see Fig. 3(b)), confirming the high intrinsic stability of the compact system.

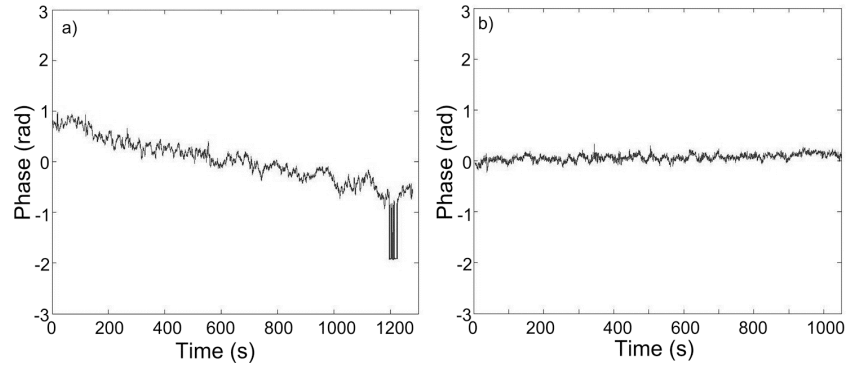


Fig. 3 a) CEP stability of the compressed output of the parametric amplifier with open feedback loop. After around 1200 s the CEP stabilization of the oscillator was switched off and on again. b) CEP stability with closed feedback loop. The phase stability corresponds to an rms noise < 70 mrad.

Furthermore the system shows a high stability of the average output power which is measured to be below 0.5 % over 100 min after a certain warm up time. The CEP and power stability measurements were performed without any active delay stabilization. This intrinsic stability was caused by the optical synchronization between signal and pump pulse, the single pass pump amplification and the completely boxed setup in combination with water cooling at several points of the system to enhance the thermal stability. Therefore this system is an ideal source for high-intensity applications such as photoionization or HHG.

3. NUMERICAL SIMULATIONS

To investigate the parametric amplification process in more detail we used a numerical model that is based on solving the nonlinear propagation equations for the ordinary and extraordinary polarized waves and includes the time dimension as well as two spatial dimensions. This enables the representation of the non-collinear propagation, including phase matching as well as walk-off and focusing/diffraction effects. Further details about the numerical simulations are given in a previous publication [20]. The parameters for the modeling of the two NOPA stages, such as beam radius, signal and pump energies, and pulse durations were taken from the experiment. As input for the first NOPA stage the measured spectral phase and amplitude from the Ti:sapphire oscillator was used. To adapt the numerics to the experimental situation the phase matching angle Θ was precisely optimized e.g. via the spectral position of a significant feature caused by the parasitic SHG. Furthermore, the delay between signal and pump pulse as well as the non-collinear angle α were adapted in the simulation to reproduce the experimentally observed spectrum. For the first NOPA stage the spectral structures as well as the spectral bandwidth match very well to the experiment for phase matching angles $\Theta = 24.35^\circ$ and $\alpha = 2.43^\circ$. As input for the modeling of the second NOPA stage, the results from the first stage are used together with the dispersion of the chirped mirrors in between both stages and the measured beam sizes. Here the phase matching angles $\Theta = 24.2^\circ$ and $\alpha = 2.36^\circ$ lead to the best match between experimental and simulated spectra with optimized temporal delay. The results from the simulation are given in Fig. 4(a) together with the measured spectrum taken from the experiment.

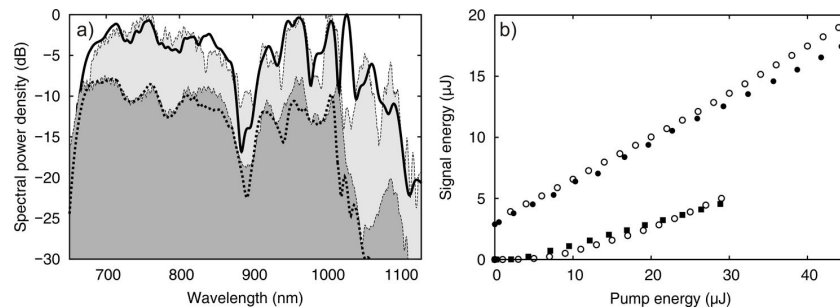


Fig. 4 a) Measured spectra obtained from the first (shaded gray) and second (shaded light gray) NOPA stage together with the calculated spectra from the numerical simulation of the first (dashed curve) and second (black curve) NOPA. b) Measured (black rectangles first NOPA, black dots second NOPA) and calculated (black circles) pulse energy after each amplification stage for different pump energies.

Furthermore, a quantitative extraction of the pulse energies from the calculations was performed. Thereby the measured beam radius of the signal is taken, and a radial symmetry of this beam is assumed. For the 27 μJ of pump energy of the first stage, the calculation denotes amplification from 1.25 nJ to 4.4 μJ which is very close to the 4.1 μJ obtained in the experiment. For the second stage the prediction from the simulation also agrees well with the experimental numbers. The slopes from the experiment and the simulations are plotted in Fig. 4(b). By the fact that the numerical model take the non-collinear interaction between signal and pump pulse into account, a detailed analysis of several spatial nonlinear mixing products, visible in the simulation and the experiment, could be performed. Further details about the comparison of spatial effects are given in our previous publication [13]. The agreement between the simulation and the experiment proves the correctness of the algorithm. The simulation code is a powerful tool to predict OPCPA performance in different situations.

4. HIGH-ORDER HARMONIC GENERATION AT HIGH REPETITION RATES

The above presented high-repetition rate OPCPA is an ideal laser source serving as workhorse for a new group of experiments in atto-science driven by high-order harmonic radiation. The high-order harmonic generation is a strongly nonlinear process and requires pulse intensities in the range of 10^{14} W/cm^2 , where tunnel ionization takes place. The efficiency of the HHG process depends on phase matching conditions [21]. Suitable laser systems for HHG so far are CPA systems available only with repetition rates up to tens of kHz. However, for experiments e.g. involving coincidence detection of two or more particles per laser shot, laser systems with a high repetition rate are more beneficial than high XUV pulse energies [16]. This applies also for time-resolved photoemission electron microscopy, where at low-repetition rate the image quality is strongly compromised by space charge effects [15, 22].

Due to the high repetition rate the pulse energy of the OPCPA is lower compared to common commercially available kHz CPA systems. Thus, for the generation of high-order harmonic radiation tight focusing is required in order to reach the sufficient intensities in the generation gas. Tight focusing results in a greatly reduced focal volume. Furthermore, very high generation gas pressure is required to achieve good phase-matching and good efficiency in tight focusing conditions [21]. Consequently, a well-designed HHG setup with elaborate differential pumping concept (see Fig. 5) must be used to fulfill the high-vacuum requirements common for attosecond experiments.

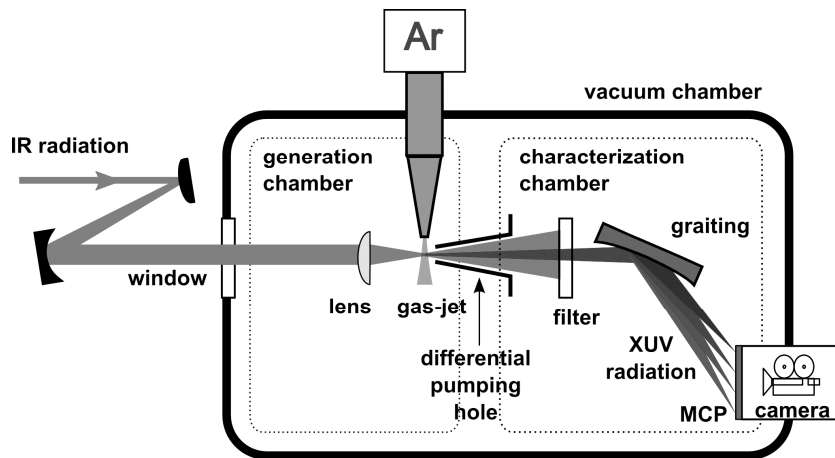


Fig. 5: Schematic HHG generation and characterization chamber including the telescope, glass window into the vacuum chamber, focusing lens, argon gas-jet, differential pumping hole, aluminum filter, XUV grating, and the MCP.

In front of the vacuum chamber the output beam diameter of the OPCPA is increased with a telescope from 2 to 5 mm. The beam enters the generation chamber through a thin window and is focused with an achromatic lens ($f = 50 \text{ mm}$) into the interaction region, defined by an argon gas jet (nozzle diameter: $90 \mu\text{m}$). The shortest possible pulse duration at the interaction region is realized through a slightly negatively chirped pulse before entering the vacuum chamber. The generation chamber and the characterization chamber are separated with a small conically expanding hole in order to enable differential pumping with a gas pressure of 10^{-2} mbar in the first chamber and 10^{-7} mbar in the second. After the generation chamber the radiation is spectrally filtered using a 200 nm thin Aluminum filter, which mainly blocks the IR pump beam from the OPCPA system. The high-order harmonic signal is detected with a homemade XUV spectrometer

based on a concave grazing incidence grating and a micro channel plate (MCP) phosphor screen combination. The phosphor screen is imaged with a CCD camera. The beam profile of the high-order harmonic beam is preserved in one spatial direction by the imaging properties of the grating. Figure 6(a) shows a harmonic spectrum as observed by the camera on the phosphor screen. With our OPCPA system typically harmonics up to energies of 46 eV are generated (see. 6(b)).

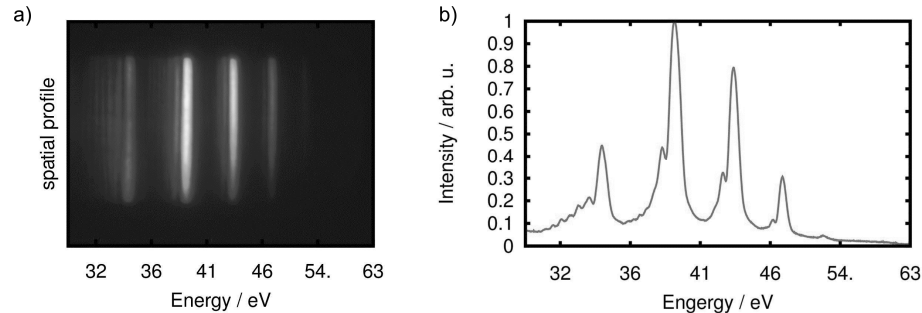


Fig. 6: High-order harmonic spectrum: a) spatially resolved image at the MCP's phosphor screen and b) spatially integrated signal.

5. CONCLUSION

In this work, an OPCPA system with high-repetition rate and few-cycle CEP-stable pulses was presented. IR pulse energies of more than 10 μJ have been generated with high conversion efficiency. Low amplitude noise below 0.5 % rms for the output power and below 70 mrad for the CEP error could be obtained due to the compact and robust system design. It was shown that the system is ideally suited for applications requiring high peak power such as HHG. For the given pump energy comparably long BBO crystals and relatively small focal sizes are required for high conversion efficiencies. In this case the PVWC geometry is favorable. Extensive numerical simulations with the model from [20] show a remarkable agreement with the experimental observations in terms of spectral shape and energy scaling.

The high-repetition rate OPCPA pulses were successfully used to drive high-order harmonic generation. XUV photon energy of up to 46 eV have been achieved. The high repetition rate HHG source presented in this work will be applied to time-resolved Photo-Emission Electron Microscopy (PEEM). Earlier experiments with a 1 kHz repetition rate XUV source revealed strong PEEM image deterioration due to space charge effects [15, 22]. Consequently, the XUV intensity had to be greatly reduced, leading to inconveniently long illumination times. The OPCPA based XUV source is 200 times faster and allows us to reduce the exposure time and consequently improve the experimentally reachable performances enormously.

Acknowledgments

This work was funded by Deutsche Forschungsgemeinschaft within the Cluster of Excellence QUEST, Centre for Quantum Engineering and Space-Time Research, within the contract Mo850/15-1, the Swedish Research Council, the Knut and Alice Wallenberg Foundation (Wallenberg Scholar), the European Research Council (Advanced Research Grant ALMA), and Stiftelsen för Strategisk Forskning.

REFERENCES

- [1] Dubietis, A., Butkus, R., and Piskarskas, A.P., "Trends in chirped pulse optical parametric amplification," *IEEE J. Sel. Topics Quantum Electron.* **12**(2), 163-172 (2006), <http://ieeexplore.ieee.org/stamp/stamp.jsp?tp=&arnumber=1632161&isnumber=34227>.
- [2] Cerullo, G., Baltuška, A., Mücke, O.D., and Vozzi, C., "Few-optical-cycle light pulses with passive carrier-envelope phase stabilization," *Laser & Photon. Rev.* **5**(3), 323-351 (2011), <http://dx.doi.org/10.1002/lpor.201000013>.
- [3] Brida, D., Manzoni, C., Cirimi, G., Marangoni, M., Bonora, S., Villoresi, P., De Silvestri, S., and Cerullo, G., "Few-optical-cycle pulses tunable from the visible to the mid-infrared by optical parametric amplifiers," *J. Opt.* **12**(1) 013001 (2010), <http://dx.doi.org/10.1088/2040-8978/12/1/013001>.
- [4] Thai, A., Hemmer, M., Bates, P., Chalus, O., and Biegert, J., "Sub-250-mrad, passively carrier-envelope-phase-stable mid-infrared OPCPA source at high repetition rate," *Opt. Lett.* **36**(19), 3918-3920 (2011), <http://dx.doi.org/10.1364/OL.36.003918>.

- [5] Shirakawa, A., Sakane, I., Takasaka, M., and Kobayashi, T., "Sub-5-fs visible pulse generation by pulse-front-matched noncollinear optical parametric amplification," *Appl. Phys. Lett.* **74**(16), 2268 (1999), <http://dx.doi.org/10.1063/1.123820>
- [6] Herrmann, D., Veisz, L., Tautz, R., Tavella, F., Schmid, K., Pervak, V., and Krausz, F., "Generation of sub-three-cycle, 16 TW light pulses by using noncollinear optical parametric chirped-pulse amplification," *Opt. Lett.* **34**(16), 2459-2461 (2009), <http://dx.doi.org/10.1364/OL.34.002459>.
- [7] Adachi, S., Ishii, N., Kanai, T., Kosuge, A., Itatani, J., Kobayashi, Y., Yoshitomi, D., Torizuka, K., and Watanabe, S., "5-fs, multi-mJ, CEP-locked parametric chirped-pulse amplifier pumped by a 450-nm source at 1 kHz," *Opt. Express* **16**(19), 14341-14352 (2008), <http://dx.doi.org/10.1364/OE.16.014341>.
- [8] Harth, A., Schultze, M., Lang, T., Binhammer, T., Rausch, S., and Morgner, U., "Two-color pumped OPCPA system emitting spectra spanning 1.5 octaves from VIS to NIR," *Opt. Express* **20**(3), 3076-3081 (2012), <http://dx.doi.org/10.1364/OE.20.003076>.
- [9] Huang, S., Cirmi, G., Moses, J., Hong, K., Bhardwaj, S., Birge, J. R., Chen, L., Li, E., Eggleton, B., Cerullo, G., and Kärtner, F. X., "High-energy pulse synthesis with sub-cycle waveform control for strong-field physics," *Nat. Photonics* **5** (8), 475-479 (2011), <http://dx.doi.org/10.1038/nphoton.2011.140>.
- [10] Thai, A., Baudisch, M., Hemmer, M., and Biegert, J., "20 μ J, few-cycle pulses at 3.1 μ m and 160 kHz repetition rate from mid-IR OPCPA," in *Conference on Lasers and Electro-Optics 2012, OSA Technical Digest (online)* (Optical Society of America, 2012), paper CM1B.2.
- [11] Schultze, M., Binhammer, T., Palmer, G., Emons, M., Lang, T., and Morgner, U., "Multi- μ J, CEP-stabilized, two-cycle pulses from an OPCPA system with up to 500 kHz repetition rate," *Opt. Express* **18**(26), 27291-27297 (2010), <http://dx.doi.org/10.1364/OE.18.027291>.
- [12] Furch, F., Birkner, S., Kelkensberg, F., Giree, A., Anderson, A., Schulz, C., and Vrakking, M., "Carrier-envelope phase stable few-cycle pulses at 400 kHz for electron-ion coincidence experiments," *Opt. Express* **21**(19), 22671-22682 (2013), <http://dx.doi.org/10.1364/OE.21.022671>.
- [13] Matyschok, J., Lang, T., Binhammer, T., Prochnow, O., Rausch, S., Schultze, M., Harth, A., Rudawski, P., Arnold, C., L'Huillier, A., and Morgner, U., "Temporal and spatial effects inside a compact and CEP stabilized, few-cycle OPCPA system at high repetition rates," *Opt. Express* **21**(24), 29656-29665 (2013), <http://dx.doi.org/10.1364/OE.21.029656>.
- [14] Rothhardt, J., Demmler, S., Hädrich, S., Limpert, J., and Tünnermann, A., "Octave-spanning OPCPA system delivering CEP-stable few-cycle pulses and 22 W of average power at 1 MHz repetition rate," *Opt. Express* **20**(10), 10870-10878 (2012), <http://dx.doi.org/10.1364/OE.20.010870>.
- [15] Mikkelsen, A., Schwenke, J., Fordell, T., Luo, G., Klunder, K., Hilner, E., Anttu, N., Zakharov, A. A., Lundgren, E., Mauritsson, J., Andersen, J. N., Xu, H. Q., and L'Huillier, A., "Photoemission electron microscopy using extreme ultraviolet attosecond pulse trains," *Rev Sci Instrum.* **80**(12), 123703 (2009), <http://dx.doi.org/10.1063/1.3263759>.
- [16] Månsson, E., Guénot, D., Arnold, C., Kroon, D., Kasper, S., Dahlström, J. M., Lindroth, E., Kheifets, A., L'Huillier, A., Sorensen, S., and Gisselbrecht, M., "Double Ionization of Xenon probed on the attosecond time scale," to be published (2013)
- [17] Krebs, M., Hädrich, S., Demmler, S., Rothhardt, J., Zaïr, A., Chipperfield, L., Limpert, J., and Tünnermann, A., "Towards isolated attosecond pulses at megahertz repetition rates," *Nat. Photonics* **7**, 555-559 (2013), <http://dx.doi.org/10.1038/nphoton.2013.131>.
- [18] Baltuška, A., Uiberacker, M., Goulielmakis, E., Kienberger, R., Yakovlev, V.S., Udem, T., Hänsch, T.W., and Krausz, F., "Phase-Controlled Amplification of Few-Cycle Laser Pulses," *IEEE J. Sel. Topics Quantum Electron.* **9**(4), 972 - 989 (2003).
- [19] Paulus, G.G., Grasbon, F., Walther, H., Villorlesl, P., Nisoll, M., Stagira, S., Priori, E., and De Silvestri, S., "Absolute-Phase phenomena in photoionization with few-cycle laser pulses," *Nature* **414**, 182-184 (2001).
- [20] Lang, T., Harth, A., Matyschok, J., Binhammer, T., Schultze, M., and Morgner, U., "Impact of temporal, spatial and cascaded effects on the pulse formation in ultra-broadband parametric amplifiers," *Opt. Express* **21**(1), 949-959 (2013), <http://dx.doi.org/10.1364/OE.21.000949>.
- [21] Heyl, C. M., Güdde, J., L'Huillier, A., and Höfer, U., "High-order harmonic generation with μ J laser pulses at high repetition rates," *J. Phys. B: At. Mol. Opt. Phys.* **45** 074020 (2012), <http://dx.doi.org/10.1088/0953-4075/45/7/074020>.
- [22] Mårsell, E., Arnold, C. L., Lorek, E., Guenot, D., Fordell, T., Miranda, M., Mauritsson, J., Xu, H., L'Huillier, A., and Mikkelsen, A., "Secondary electron imaging of nanostructures using Extreme Ultra-Violet attosecond pulse trains and Infra-Red femtosecond pulses," *Ann. Phys.* **525**(1-2), 162-170 (2013), <http://dx.doi.org/10.1002/andp.201200269>.